Inorganic Chemistry

Article

pubs.acs.org/IC

Hydrothermal Synthesis and Crystal Structure of Two New Hydrated Alkaline Earth Metal Borates $Sr_3B_6O_{11}(OH)_2$ and $Ba_3B_6O_{11}(OH)_2$

Carla Heyward, Colin McMillen, and Joseph Kolis*

Department of Chemistry and Center for Optical Materials Science and Engineering Technologies (COMSET), Clemson University, Clemson, South Carolina 29634, United States

Supporting Information

ABSTRACT: Two new hydrated borates $Sr_3B_6O_{11}(OH)_2$ (**1**) and $Ba_3B_6O_{11}(OH)_2$ (**2**) were hydrothermally synthesized. Their structures were determined by single-crystal X-ray diffraction and further characterized by IR, powder XRD, and DSC/TGA. Compound **1** crystallizes in the triclinic space group $P\bar{1}$ with unit cell parameters of a = 6.6275(13) Å, b = 6.6706(13) Å, c = 11.393(2) Å, α = 91.06(3)°, β = 94.50(3)°, and γ = 93.12(3)°, while compound **2** crystallizes in the noncentrosymmetric monoclinic space group Pc with a = 6.958(14) Å, b = 7.024(14) Å, c = 11.346(2) Å, and β = 90.10(3)°. In spite of the differences in symmetry and packing of the borate chains, both structures consist of the same fundamental building block (FBB) of a $[B_6O_{11}(OH)_2]^{-6}$ unit and three unique alkaline earth metal atoms.

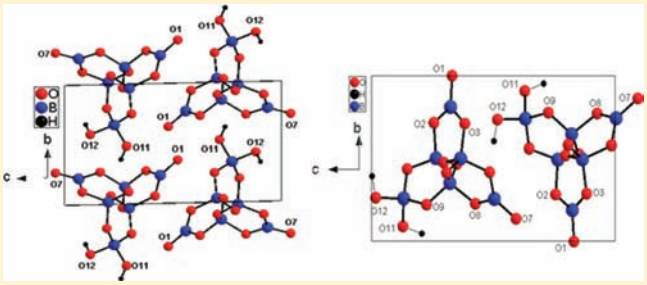

INTRODUCTION

Metal borates possess a number of interesting crystal properties that make them attractive for nonlinear optical (NLO) applications. Boron has two different basic coordination environments with oxygen: trigonal planar and tetrahedral. These polyhedra can be combined in varying ratios to form an almost infinite variety of different types of fundamental building blocks (FBBs) including rings, chain of rings, sheets, and frameworks. As a result, metal borates offer rich descriptive structural chemistry.[1−3]

The boron−oxygen polyhedra themselves lack a center of symmetry, and borates have a statistically higher average of formation of noncentrosymmetric solid structures. Thus, only 15% of all inorganic materials are noncentrosymmetric, whereas 36% of inorganic borate structures form in noncentrosymmetric space groups, making them potential NLO materials.[4,5] Metal borates also tend to have exceptionally wide transparency ranges, with some having band edges as low as 155 nm.[6] They also typically have higher optical damage thresholds and excellent chemical and thermal stability. These factors combine to make them very attractive for NLO applications in UV and deep UV regions.[3] Thus, single crystals such as KBBF,[7] β-BaB_2O_4 (BBO), and LiB_3O_5 (LBO) are well-known NLO materials used for laser manipulations in the UV region.[5,8−10] These materials, however, have a number of shortcomings that limit their performance in UV and deep UV NLO applications. Therefore, further research is still needed to synthesize new and improved metal borate structures.[4]

Metal borates are commonly grown by the flux method, which can produce well-defined crystals, but application of flux growth can be limited due to formation of glassy products. We found that hydrothermal synthesis is an efficient alternative method for growth of high optical quality metal borate single crystals, in particular those having modest thermal stabilities. We demonstrated that a wide variety of metal borates could be grown as high-quality single crystals. The chemistry is very versatile and flexible, so a wide range of phase space can be developed.[6,11−13] A particularly rich area of chemistry is the borates of strontium and barium that have an exceptionally rich descriptive chemistry in hydrothermal fluids. Our original efforts were prompted by a desire to prepare single crystals of MB_2O_4 as structural analogs to the commercially important β-BaB_2O_4 (BBO). Unfortunately we have seen no evidence of growth of BBO but rather the preferred formation of a wide variety of metal borates containing the B−OH moiety. Since the descriptive chemistry is very extensive and many of these compounds are noncentrosymmetric, the class serves as an excellent exploratory exercise. Furthermore, the noncentrosymmetric structures serve as an inspiration for other borates with the OH groups to be replaced with halides (see accompanying paper in this issue).

This paper describes the synthesis and crystal structures of two new hydrated strontium and barium borate compounds. Despite having the same nominal chemical formula and essentially the same fundamental building block, they have very different packing with one in a centrosymmetric and the other in a noncentrosymmetric space group, making it a possible nonlinear material. These results give a hint of the very

Received: October 26, 2011
Published: March 12, 2012

   dx.doi.org/10.1021/ic202316t | *Inorg. Chem.* 2012, 51, 3956−3962

extensive crystal chemistry of metal borates as hydrothermal growth continues to provide a rich source of new compounds.

EXPERIMENTAL SECTION

Synthesis. Feedstock for crystal growth for $Sr_3B_6O_{11}(OH)_2$ (**1**) was first prepared by a solid state melt of 1.06 g (44 mmol) of LiOH (Aldrich, 98%), 3.06 g (43 mmol) of B_2O_3 (Alfa Aesar, 98%), 5.82 g (22 mmol) of $Sr(OH)_2{\cdot}8H_2O$ (Aldrich, 95%), and 1.23 g (22 mmol) of KOH (MV laboratories, 99%). The powders were thoroughly mixed and heated in a platinum crucible at 900 °C in air for 16 h to produce a crystalline starting material.

Single crystals of $Sr_3B_6O_{11}(OH)_2$ (**1**) were formed by spontaneous nucleation in silver ampules 0.25 in. diameter and 2.5 in. in length. The feedstock (0.1 g) prepared above along with 0.4 mL of 0.5 M $SrCl_2$ mineralizer solution were welded shut in the ampules. The ampules were placed in a Tuttle cold seal autoclave with the remaining volume filled with water and heated for 6 days at 560 °C generating about 18 kpsi of pressure. After the autoclaves were cooled, the ampules were removed from the autoclave and the crystalline products were washed with deionized water and air dried. Colorless rods up to 0.95 mm in size of $Sr_3B_6O_{11}(OH)_2$ were formed in approximately 90% yield with tetragonal $LiBO_2$ forming as a side product. Use of 2 M LiCl and 1 M KCl as a mineralizer solution decreased the yield of the target phase in favor of $LiBO_2$.

$Ba_3B_6O_{11}(OH)_2$ (**2**) was synthesized using the same reaction conditions but through a direct hydrothermal reaction of separate precursor powders. This reaction had a starting charge of 260 mg (0.86 mmol) of $K_2B_4O_7{\cdot}4H_2O$ (Aldrich, 99.5%), 20 mg (0.32 mmol) of H_3BO_3 (Fisher, 99%), and 10 mg (0.055 mmol) of $Ba(OH)_2{\cdot}H_2O$ (Aldrich, 99.9%) and used 0.4 mL of 1 M NaOH mineralizer. Clear, colorless needles up to 1.5 mm in size were formed in approximately 95% yield.

Structure Determination. A suitable crystal (0.2 mm × 0.2 mm × 0.15 mm) of compound **1** was carefully mounted on a glass fiber using epoxy glue. The crystal was placed on a Rigaku AFC8 diffractometer equipped with a Mercury CCD detector and an X-ray source using graphite monochromated Mo Kα (λ = 0.71073 Å) radiation. The final unit cell constants of the structures were determined by least-squares refinement using SHELXTL-97 software.[14] The structure of compound **2** was determined similarly with a 0.08 mm × 0.10 mm × 0.15 mm size crystal.

The structure of $Sr_3B_6O_{11}(OH)_2$ was determined in the triclinic space group $P\bar{1}$ with unit cell parameters of a = 6.6275(13) Å, b = 6.6706(13) Å, c = 11.393(2) Å, α = 91.06(3), β = 94.50(3)°, and γ = 93.12(3)°. A total of 4794 reflections were collected, of which 2034 were unique. All non-hydrogen atoms were refined anisotropically. One atom (B1) exhibited nonpositive definite anisotropic mean square displacements, so restraints were placed on this atom in the final refinement using the ISOR command of SHELXTL. An additional symmetry check was done by solving $Sr_3B_6O_{11}(OH)_2$ in space group $P1$, but the PLATON for Windows software program suggested a higher symmetry of $P\bar{1}$ and not Pc.[15]

The structure of $Ba_3B_6O_{11}(OH)_2$ was determined in the non-centrosymmetric monoclinic space group Pc, with unit cell parameters of a = 6.9580(13) Å, b = 7.0240(14) Å, c = 11.346(2) Å, and β = 90.10(3)°. A total of 4558 reflections were collected, 1940 of which were unique. Additional crystallographic data and structure refinements are summarized in Table 1. Although attempts were made to solve $Ba_3B_6O_{11}(OH)_2$ in more common space groups such as $P\bar{1}$ and $P2_1/c$, Pc was the only space group in which a reliable solution could be obtained. As confirmation of the space group choice, the structure was also determined assuming no symmetry in space group $P1$ and then checked for higher symmetry using the PLATON software package.[15] PLATON verified the choice of Pc as the space group in spite of an unusually high Flack parameter of 0.41(3). This is likely due to partial crystal twinning in the needle used for data collection, so a TWIN refinement was applied resulting in a final R_1 value of 0.0237. All non-hydrogen atoms were refined anisotropically, but B2, B3, and B4 were refined using the ISOR restraint due to their unusually low mean square anisotropic displacement parameters. Hydrogen atoms in compounds **1** and **2** were located by inspecting the local oxygen environments and calculating the bond valence of each oxygen atom.

Table 1. Crystallographic Data for New Hydrated Alkaline Earth Borates

empirical formula	$Sr_3B_6O_{11}(OH)_2$ (**1**)	$Ba_3B_6O_{11}(OH)_2$ (**2**)
fw	537.74	686.90
space group	$P\bar{1}$ (no. 2)	Pc (no. 7)
a, Å	6.6275 (13)	6.958 (14)
b, Å	6.6706 (13)	7.024 (14)
c, Å	11.393 (2)	11.346 (2)
α, deg	91.06 (3)	90
β, deg	94.50(3)	90.10 (3)
γ, deg	93.12 (3)	90
V, Å^3	501.26 (17)	554.51 (15)
Z	2	2
D_{calcd}, Mg/m^3	3.563	4.114
parameters	200	201
μ, mm^{-1}	15.985	10.609
θ range, deg	3.06–26.38	2.90–25.25
reflns collected	4794	4558
reflns independent	2034	1940
reflns obs [$I \geq 2\sigma(I)$]	1828	1919
R(int)	0.0288	0.0369
final R (obs data)[a]		
R_1	0.0273	0.0237
wR_2	0.0612	0.0563
final R (all data)		
R_1	0.0316	0.0243
wR_2	0.0631	0.0565
goodness of fit on F^2	1.11	1.12
largest diff. peak, e/Å^3	0.99	0.81
largest diff. hole, e/Å^3	−1.38	−0.93

[a] $R_1 = [\sum||F_o| - |F_c||]/\sum|F_o|$; $wR_2 = \{[\sum w[(F_o)^2 - (F_c)^2]^2]\}^{1/2}$.

Additional Characterization. Powder X-ray diffraction patterns of finely ground crystals of both compounds were characterized using a Rigaku Ultima IV powder diffractometer equipped with Cu Kα radiation (λ = 1.5418 Å) in the angular range from 5° to 60° 2θ with a scanning step size of 0.02°. A simulated pattern generated from the single-crystal data using the PLATON software package was used as comparison to the experimental powder patterns.[15]

Infrared spectroscopy was recorded using the KBr pellet technique under flowing nitrogen on a Nicolet Magna 550 IR spectrometer. Spectra of the title compounds were collected in the range of 400–4000 cm^{-1}. Thermogravimetric analysis was performed using a TA Instruments SDT2960 simultaneous DSC/TGA. Weight loss for both compounds was measured upon heating to 1000 °C at 10°/min in a nitrogen atmosphere.

RESULTS AND DISCUSSION

Crystal Structures. The crystal structure of $Sr_3B_6O_{11}(OH)_2$ (**1**) consists of three crystallographically distinct strontium atoms and a $[B_6O_{11}(OH)_2]^{-6}$ polyborate anion. According to the notation proposed by Hawthorne, Burns, and Grice, the FBB shown in Figure 1a can be written as $\langle 3\square\rangle{-}\langle\Delta 2\square\rangle\Delta$ which consists of a triangular tail attached to two orthogonal six-membered rings which share a common boron atom.[1,16] The $Ba_3B_6O_{11}(OH)_2$ (**2**) structure also has three crystallographically unique barium atoms and a $[B_6O_{11}(OH)_2]^{-6}$ asymmetric unit shown in Figure 1b. The FBBs of the two compounds are identical in their constituent borates (with the orthogonal rings built of a BO_3 group and four BO_4 groups), but we do note orientational differences in the FBBs. This is

dx.doi.org/10.1021/ic202316t | Inorg. Chem. 2012, 51, 3956–3962

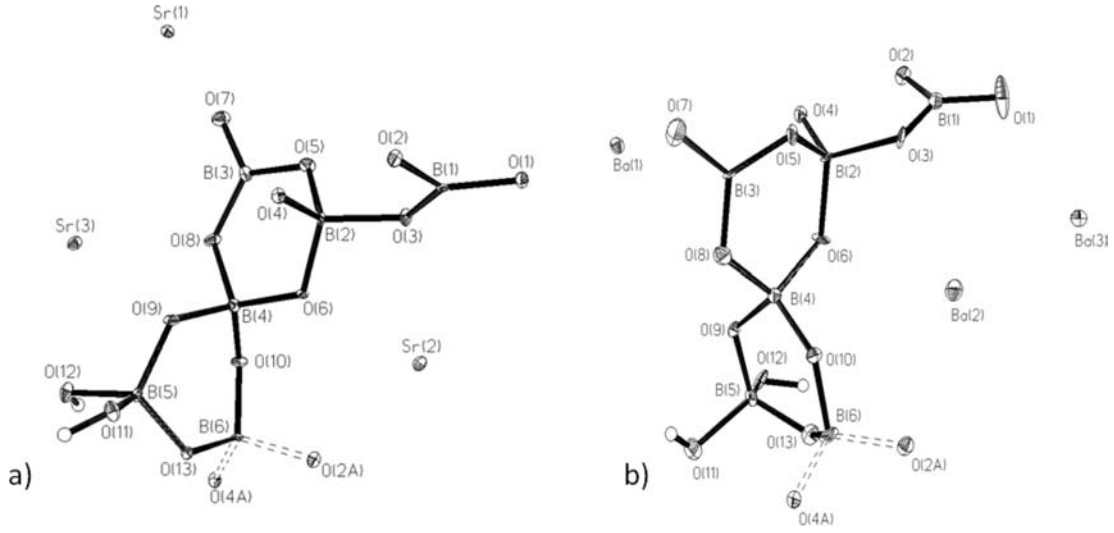

Figure 1. Extended $[B_6O_{11}(OH)_2]^{-6}$ unit of (a) $Sr_3B_6O_{11}(OH)_2$ and (b) $Ba_3B_6O_{11}(OH)_2$ as 50% probability thermal ellipsoids.

particularly evident in the directionalities of the B2−O4 and B5−O12 bonds relative to the other atoms in the FBB. With the help of the different metal cation (also having slightly different connectivities for Sr vs Ba), the orientational differences in the FBBs result in a different overall structure and packing arrangement in compounds **1** and **2**.

The B−O bond distances in the triangular borate groups range from 1.334 (5) to 1.414 (5) Å for both compounds, with an average of 1.382 (compound **1**) and 1.378 Å (compound **2**), while the O−B−O angles range from 116.9(8)° to 123.0(8)°. Corresponding bond distances for the tetrahedral borate groups range from 1.420 (5) to 1.527 (5) Å with an average of 1.476 (compound **1**) and 1.474 Å (compound **2**) with bond angles ranging from 104.5(6)° to 113.0(7)°. These are in agreement with reported average B−O distances and O−B−O angles for structures where both borate groups coexist.[17,18] Selected bond distances and angles are listed in Tables 2 and 3. Both structures exhibit a slight elongation in tetrahedral B−O bonds that bridge to triangular boron atoms, as the triangular boron atoms tend to pull shared oxygen atoms away from the tetrahedral boron atom, probably due to a small amount of π bonding for the trigonal borates.

In the $Sr_3B_6O_{11}(OH)_2$ structure, the $[B_6O_{11}(OH)_2]^{-6}$ polyborate framework links with other FBBs through ring formation of B1−O3−B2−O4−B6−O2 to form chains which polymerize in the [100] direction as shown in Figure 2. There are two chains per unit cell that are related by an inversion center clearly visible in Figure 3a. Polarity in the borate chains is eliminated by the borate bonds B1−O1 and B3−O7 pointing in different directions, resulting in a nonpolar framework.[19] The chains in $Ba_3B_6O_{11}(OH)_2$ likewise extend infinitely along [100] by B1−O2−B6 and B2−O4−B6 bonding shown in Figure 2. This bonding results in formation of three approximately orthogonal rings that are repeated as the chain propagates.

There are two such chains per unit cell, each related by the *c*-glide perpendicular to the *b* axis. As such, the chains are mirror images of one another with respect to the *b* axis but maintain the same polarity along [001], also evident in Figure 3b. This is most obvious in the directionality of the B5−O12 and B3−O7 bonds with respect to the *c* axis.

The strontium ions in compound **1** have two different coordination environments of eight and nine shown in Figure 4. Sr1 is coordinated to nine framework oxygen atoms with an average Sr−O distance of 2.671 Å. Sr1−O12 has a longer bond of 3.263 (3) Å, resulting in a severely distorted polyhedron.[20,21] Sr1 is corner sharing through O13 and edge sharing through O1, O3, and O11 with Sr2. Sr1 is also edge sharing with Sr3 through O7−O9 and O5−O12. Sr2 and Sr3 are eight-coordinated polyhedra with an average bond distance of 2.620 Å, forming an irregular polyhedron.[20] Sr2 and Sr3 do not share any oxygen atoms with each other and are always separated by Sr1 atoms. On an interesting note, O4 is only bonded to Sr1 and O10 is only bonded to Sr3. This type of oxygen bonding is not present in compound **2**.

In compound **2**, the barium ions have a complicated structural arrangement; the coordination environments are displayed in Figure 4. Ba1 forms a nine-coordinate polyhedron with an average Ba−O bond distance of 2.817 Å but has a slightly longer Ba−O7 bond of 3.118 (6) Å.[21] Ba1 is corner sharing through O2, O7, O8, and O10 with Ba2 and edge sharing through O1−O4, O5−O13, and O7−O11 edges with Ba3 polyhedra. Ba2 forms an eight-coordinate polyhedron with an average Ba−O bond distance of 2.838 Å. Unlike compound **1**, Ba2 and Ba3 polyhedra are edge sharing through O3−O12 and O7−O9 edges as well as corner sharing through O6. Ba3 is coordinated to 10 framework oxygen atoms with an average bond distance of 2.874 Å but has a longer Ba3−O1 bond of 3.245 (7) Å.[21] In this arrangement, O7 serves as a common vertex for all three unique Ba atoms. This common oxygen vertex with all three unique Sr atoms is absent in compound **1**. Ba−O bond distances range from 2.706 (7) to 3.245 (7) Å. Thus, in order to accommodate the larger Ba^{2+} ions in this complex arrangement, the $[B_6O_{11}(OH)_2]^{-6}$ chain structure of **2** is slightly modified from that in **1** and results in an overall noncentrosymmetric arrangement.

Hydrogen atom assignment was necessary in order to satisfy charge balance and bond valence considerations for both structures. For $Sr_3B_6O_{11}(OH)_2$, the unique hydrogen atoms H11 and H12 were assigned to O11 and O12 by identifying these oxygen atoms as underbonded (1.15 and 1.22 vu). The location of these hydrogen atoms was identified from residual electron density 0.888 (3) and 0.966 (3) Å away from O11 and O12, respectively.[22,23] For $Ba_3B_6O_{11}(OH)_2$, after assignment of all non-hydrogen atoms there were again two areas of residual

dx.doi.org/10.1021/ic202316t | *Inorg. Chem.* 2012, 51, 3956−3962

Table 2. Selected Bond Distances (Angstroms) and Angles (degrees) for $Sr_3B_6O_{11}(OH)_2$ (1)[a]

BO_3 group				
	distances	BVS		angles
B1–O1[5]	1.335 (5)	1.10	O1[5]–B1–O2[6]	118.4 (4)
B1–O2[6]	1.414 (5)	0.90	O1[5]–B1–O3[8]	122.3 (4)
B1–O3[8]	1.407 (6)	0.91	O2[6]–B1–O3[8]	119.2 (4)
B3–O5	1.403 (6)	0.92	O5–B3–O7	119.8 (4)
B3–O7	1.334 (5)	1.11	O7–B3–O8[2]	121.4 (4)
B3–O8[2]	1.398 (5)	0.93	O5–B3–O8[2]	118.8 (3)
BO_4 group				
	distances	BVS		angles
B2–O3	1.507 (5)	0.69	O4–B2–O3	111.8 (3)
B2–O4	1.420 (5)	0.88	O6–B2–O3	107.7 (3)
B2–O5[2]	1.526 (5)	0.75	O5[2]–B2–O3	106.1 (3)
B2–O6	1.450 (5)	0.81		
B4–O6	1.445 (5)	0.82	O6–B4–O9[9]	111.2 (3)
B4–O8	1.517 (5)	0.68	O8–B4–O9[9]	106.4 (3)
B4–O9[9]	1.485 (5)	0.73	O10–B4–O9[9]	111.0 (3)
B4–O10	1.456 (5)	0.80		
B5–O9	1.452 (5)	0.80	O11–B5–O9	107.2 (4)
B5–O11	1.491 (5)	0.72	O12–B5–O9	108.9 (3)
B5–O12	1.507 (5)	0.69	O13[5]–B5–O9	112.2 (3)
B5–O13[5]	1.462 (5)	0.78		
B6–O2	1.527 (5)	0.66	O4[10]–B6–O13	106.6 (3)
B6–O4[10]	1.430 (6)	0.85	O10[6]–B6–O13	111.7 (3)
B6–O10[6]	1.453 (5)	0.80	O2–B6–O13	108.6 (3)
B6–O13	1.489 (5)	0.73		

SrO_8			SrO_9		
	distances	BVS		distances	BVS
Sr2–O1	2.548 (3)	0.31	Sr1–O1	2.617 (3)	0.26
Sr2–O1[5]	2.656 (3)	0.23	Sr1–O3	2.700 (3)	0.21
Sr2–O2[6]	2.734 (3)	0.19	Sr1–O4[1]	2.424 (3)	0.44
Sr2–O2	2.639 (3)	0.25	Sr1–O5[2]	2.649 (3)	0.21
Sr2–O3	2.727 (3)	0.19	Sr1–O7	2.643 (3)	0.24
Sr2–O6	2.465 (3)	0.39	Sr1–O9	2.545 (3)	0.32
Sr2–O11	2.686 (3)	0.22	Sr1–O11	2.699 (3)	0.21
Sr2–O13	2.499 (3)	0.36	Sr1–O12[4]	3.263 (3)	0.05
Sr3–O5	2.617 (3)	0.26	Sr1–O13[3]	2.499 (3)	0.22
Sr3–O7	2.573 (3)	0.29			
Sr3–O8[1]	2.643 (3)	0.24			
Sr3–O8[7]	2.802 (3)	0.16			
Sr3–O9	2.554 (3)	0.31			
Sr3–O10[7]	2.463 (3)	0.39			
Sr3–O12	2.740 (3)	0.29			
Sr3–O12[7]	2.574 (3)	0.19			

[a]Symmetry codes: (1) $x, y + 1, z$; (2) $-x + 1, -y + 1, -z + 2$; (3) $-x + 1, -y + 1, -z + 1$; (4) $x + 1, y, z$; (5) $-x, -y + 1, -z + 1$; (6) $-x, -y, -z + 1$; (7) $-x, -y + 1, -z + 2$; (8) $x - 1, y, z$; (9) $x, y - 1, z$; (10) $-x + 1, -y, -z + 1$.

electron density 0.939 (1)–0.939 (0) Å away from both O11 and O12, atoms which would otherwise be extremely underbonded.[22,23] H11 and H12 were assigned to these respective oxygen atoms. Hydrogen bonding likely occurs in both structures. For compound **1**, the weaker O12–H12···O7 hydrogen bond is 1.77 Å along the [001] direction (for a total hydrogen bond length of 2.74 Å).[24] Because of the slightly different relative orientations of the OH^- groups in the title compounds, the hydrogen bonding in compound **2** occurs between the chains by connecting the chains along the [010] direction through O11–H11···O1 interactions.[24] The total hydrogen-bond length here is 2.87 Å. Both H12–O7 (in **1**) and H11–O1 (1.93 Å in **2**) distances are reasonable if the oxygen

Table 3. Selected Bond Distances (Angstroms) and Angles (degree) for $Ba_3B_6O_{11}(OH)_2$ (2)[a]

BO_3 group				
	distances	BVS		angles
B1–O1	1.338 (12)	1.09	O1–B1–O2	121.3 (9)
B1–O2	1.373 (13)	1.00	O1–B1–O3[5]	118.9 (9)
B1–O3[5]	1.402 (12)	0.92	O2–B1–O3[5]	119.8 (8)
B3–O5[13]	1.410 (11)	0.90	O5[13]–B3–O7	120.1 (9)
B3–O7	1.356 (13)	1.04	O5[13]–B3–O8	116.9 (8)
B3–O8	1.389 (13)	0.95	O7–B3–O8	123.0 (8)
BO_4 group				
	distances	BVS		angles
B2–O3[6]	1.502 (12)	0.70	O3[6]–B2–O6	109.3 (7)
B2–O4	1.454 (11)	0.80	O4–B2–O6	111.1 (7)
B2–O5[12]	1.484 (12)	0.74	O5[12]–B2–O6	110.8 (7)
B2–O6	1.439 (11)	0.83		
B4–O6	1.465 (10)	0.78	O6–B4–O9	111.2 (6)
B4–O8[3]	1.508 (10)	0.69	O8[3]–B4–O9	104.5 (6)
B4–O9	1.447 (11)	0.82	O9–B4–O10[3]	113.0 (7)
B4–O10[3]	1.465 (10)	0.78		
B5–O9[1]	1.450 (14)	0.81	O9[1]–B5–O11	106.3 (7)
B5–O11	1.514 (12)	0.68	O9[1]–B5–O12[9]	110.4 (9)
B5–O12[9]	1.474 (13)	0.76	O9[1]–B5–O13[2]	112.9 (8)
B5–O13[2]	1.477 (12)	0.75		
B6–O2[2]	1.507 (12)	0.69	O2[2]–B6–O4	110.5 (7)
B6–O4	1.450 (12)	0.81	O4–B6–O10[4]	109.2 (8)
B6–O10[4]	1.489 (12)	0.73	O4–B6–O13[2]	112.3 (8)
B6–O13[2]	1.451 (11)	0.81		

BaO_8			BaO_9		
	distances	BVS		distances	BVS
Ba2–O2	2.823 (6)	0.23	Ba1–O1[9]	2.714 (7)	0.31
Ba2–O3	2.810 (7)	0.24	Ba1–O2	2.855 (7)	0.21
Ba2–O6[13]	2.821 (6)	0.24	Ba1–O4[9]	2.788 (7)	0.26
Ba2–O7	2.732 (6)	0.30	Ba1–O5[10]	2.716 (6)	0.31
Ba2–O8[4]	3.000 (7)	0.15	Ba1–O7[5]	3.118 (6)	0.11
Ba2–O9[1]	2.719 (6)	0.31	Ba1–O8	2.880 (6)	0.20
Ba2–O10[14]	3.084 (6)	0.12	Ba1–O10	2.744 (5)	0.29
Ba2–O12	2.713 (6)	0.32	Ba1–O11	2.684 (7)	0.34
			Ba1–O13	2.855 (6)	0.21

BaO_{10}		
	distances	BVS
Ba3–O1[9]	3.245 (7)	0.08
Ba3–O3[8]	2.745 (7)	0.29
Ba3–O4	2.706 (7)	0.32
Ba3–O5	2.798 (6)	0.25
Ba3–O6	2.781 (6)	0.26
Ba3–O7[5]	2.799 (6)	0.25
Ba3–O9	2.759 (6)	0.28
Ba3–O11	2.821 (7)	0.24
Ba3–O12[8]	2.984 (6)	0.15
Ba3–O13[2]	3.098 (6)	0.11

[a]Symmetry codes: (1) $x + 1, y, z$; (2) $x, y + 1, z$; (3) $x - 1, -y + 2, z - 1/2$; (4) $x, -y + 2, z - 1/2$; (5) $x - 1, y, z$; (6) $x - 1, y + 1, z$; (7) $x, -y + 1, z + 1/2$; (8) $x - 1, -y + 2, z + 1/2$; (9) $x, -y + 2, z + 1/2$; (10) $x, y - 1, z$; (11) $x + 1, -y + 2, z - 1/2$; (12) $x, -y + 3, z - 1/2$; (13) $x + 1, y - 1, -z$; (14) $x, -y + 1, z - 1/2$; (15) $x + 1, -y + 2, z + 1/2$; (16) $x, -y + 3, z + 1/2$.

dx.doi.org/10.1021/ic202316t | Inorg. Chem. 2012, 51, 3956–3962

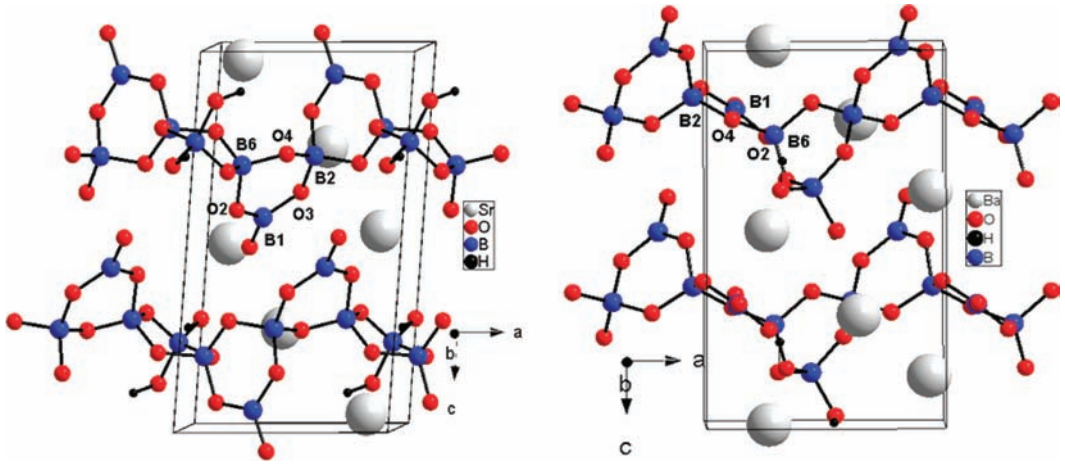

Figure 2. Packing of the metal atoms within the borate chains looking down the *b* axis.

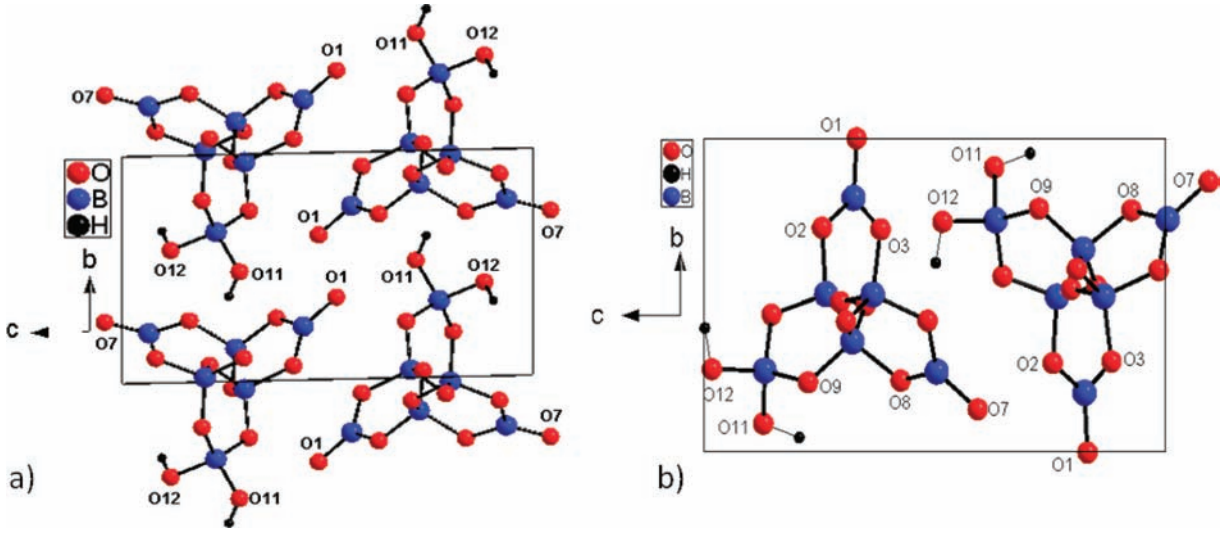

Figure 3. (a) $Sr_3B_6O_{11}(OH)_2$ centrosymmetric borate chains and (b) $Ba_3B_6O_{11}(OH)_2$ noncentrosymmetric borate chains both along [100] direction.

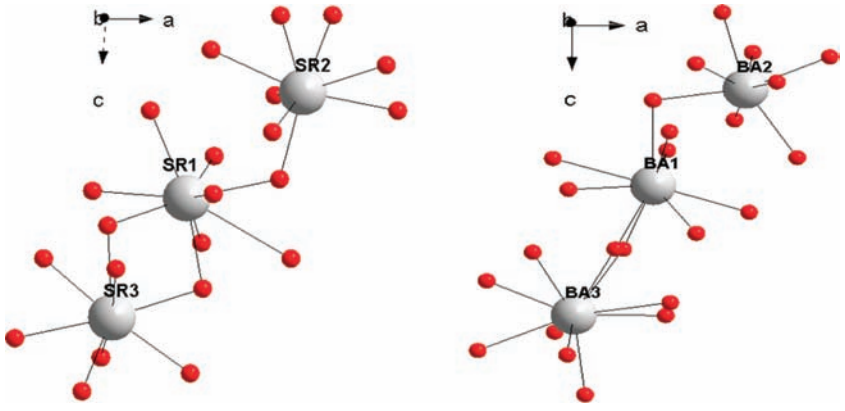

Figure 4. Alkaline earth metal coordination environments slightly off the *b* axis.

atoms act as hydrogen-bond acceptors. In fact, such a donor–acceptor relationship is helpful to satisfy the bond valences for all oxygen atoms in question. The other hydrogen atoms H11 in compound **1** and H12 in compound **2** do not appear to participate in extended hydrogen bonding. A bond valence analysis of both compounds **1** and **2** is included in Tables 2 and 3 using the parameters of Brese and O'Keeffe.[25]

Powder XRD. The powder XRD patterns of compounds **1** and **2** are compared to their simulated patterns from the crystallographic data of $Sr_3B_6O_{11}(OH)_2$ and $Ba_3B_6O_{11}(OH)_2$ (Figure 5). The experimental powder XRD pattern of compound **1** is in agreement with the simulated pattern except for one minor peak at approximately 25° associated with the $LiBO_2$ phase. The experimental pattern of compound **2** is

dx.doi.org/10.1021/ic202316t | *Inorg. Chem.* 2012, 51, 3956–3962

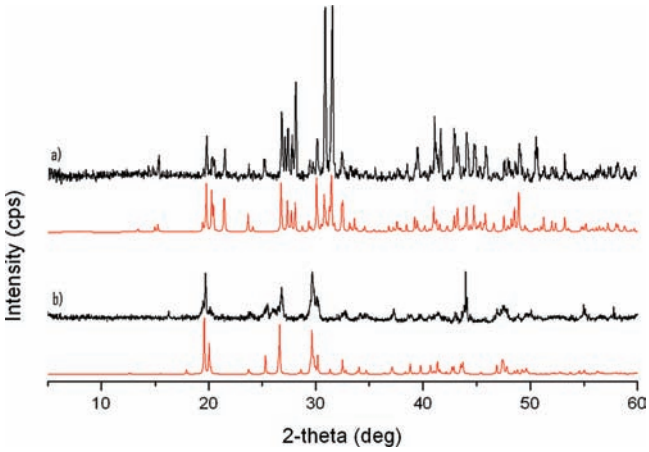

Figure 5. Powder X-ray diffraction patterns of (a) experimental data (black) compared to simulated pattern (red) for **1**. Minor peak at ~25° corresponds to $LiBO_2$. (b) Experimental data (black) compared to simulated pattern (red) for **2**.

consistent with the simulated pattern, indicating the absence of any impurities in the sample. The experimental patterns are noticeably different, which supports the different space group determination of **1** and **2**.

Infrared Spectroscopy. Infrared spectroscopic analysis (Figure 6) was performed to validate the existence of the hydroxyl group as well as the different borate groups in the crystal structures. The IR spectrum for compound **1** exhibits a broad band at 3437 cm^{-1} to support the presence of hydroxyl

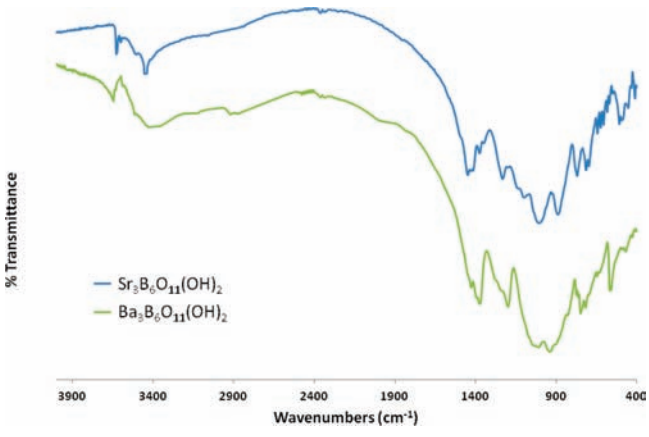

Figure 6. Infrared spectra of compounds **1** and **2**.

groups in the structure.[26−28] The bands in the range of 1441−1333 cm^{-1} correspond to the B−O stretching vibrations of triangular borate groups in the presence of tetrahedral borate groups, whereas those in the range of 1116−692 cm^{-1} are attributable to the tetrahedral borate groups in the presence of triangular borate groups.[26−28] Additional B−OH and B−O bending modes are present at 1220 and 476−406 cm^{-1}, respectively.[26−28] For compound **2**, peaks in the range of 1423−1370 and 1050−640 cm^{-1} are characteristic for triangular and tetrahedral borates, respectively. The broad hydroxide stretch was also observed around 3360 cm^{-1}. The B−OH and B−O bending modes are in the same region as compound **1** as expected.

Thermogravimetric Analysis. Thermogravimetric analysis for $Sr_3B_6O_{11}(OH)_2$ indicated a weight loss of 2.7% from 50 to 700 °C. Theoretical weight loss for H_2O in compound **1** was 3.3%. For $Ba_3B_6O_{11}(OH)_2$, a total weight loss of 3.2% was observed from 50 to 700 °C as well. Theoretical weight loss for H_2O in compound **2** was 2.6%. These results imply that the crystals are unstable with respect to loss of water. We are not sure of the cause of the additional minor weight loss in **2**, but decomposition of a hydroxylated crystal lattice with respect to water loss at moderate temperatures is not unexpected. Combined with a high thermo-optic coefficient associated with OH-containing species, the potential breakdown of these hydrated materials in high power (generating higher temperatures) systems makes these species less desirable for optical applications.

CONCLUSIONS

In summary, our work describes the hydrothermal synthesis and crystal structure of two new hydrated alkaline earth metal borates, $Sr_3B_6O_{11}(OH)_2$ (**1**) and $Ba_3B_6O_{11}(OH)_2$ (**2**). Both structures consist of a large $[B_6O_{11}(OH)_2]^{-6}$ unit that polymerizes to create independent borate chains. Despite the similar formulas, the two compounds have very different crystal structures with compound **1** forming in the centrosymmetric space group *P*−1 and compound **2** crystallizing in a noncentrosymmetric space group *Pc*. In compound **1** the inversion center is clearly visible, while the noncentrosymmetry in compound **2** is noticeable due to the polarity of the borate chains. The larger alkaline earth metal atoms also contribute to decidedly different packing within the unit cell. These subtle differences in the orientation of the borate framework result in the very different space groups for the two compounds, and the different structures are also apparent in the observed powder XRD profiles and IR spectra. Our results demonstrate that introducing alkaline earth metals into the borate system can continue to produce interesting new borate materials including those with noncentrosymmetric space groups.

It appears that unless other steps are taken in the chemistry, the hydroxylated species will continue to dominate the alkaline earth borates when grown from hydrothermal solutions. Crystals containing hydroxylated borates are unstable compared to anhydrous borates or those containing other coordinating ions such as F^-. The presence of hydroxyl groups typically results in a high thermo-optic coefficient which can affect phase matching or in a worst-case scenario result in decomposition of the crystal at higher operating temperatures. This makes them poor candidates for nonlinear optical crystals or laser host materials. However, the richness of the structural chemistry of metal borates allows small changes in the reaction conditions to lead to new products; therefore, future exploratory research will be devoted to synthesizing new noncentrosymmetric materials and eliminating the hydroxyl group from the crystal lattice or replacing them with more suitable ions such as F^-.

ASSOCIATED CONTENT

Supporting Information

Single crystal data is provided in CIF format. This material is available free of charge via the Internet at http://pubs.acs.org.

AUTHOR INFORMATION

Corresponding Author

*E-mail: kjoseph@clemson.edu.

Notes

The authors declare no competing financial interest.

■ ACKNOWLEDGMENTS

We are grateful for the generous financial support of this work from the National Science Foundation (DMR-0907359).

■ REFERENCES

(1) Burns, P. C.; Grice, J. D.; Hawthorne, F. C. *Can. Mineral* **1995**, *33*, 1131.
(2) Christ, C. L.; Clark, J. R. *Phys. Chem. Miner.* **1977**, *2*, 59.
(3) Becker, P. *Adv. Mater.* **1998**, *10*, 979.
(4) Chen, C.; Lin, Z.; Wang, Z. *Appl. Phys. B: Laser Opt.* **2005**, *80*, 1.
(5) Aka, G.; Brenier, A. *Opt. Mater.* **2003**, *22*, 89.
(6) McMillen, C.; Giesber, H.; Kolis, J. *J. Cryst. Growth* **2008**, *310*, 299.
(7) McMillen, C.; Hu, J.; VanDerveer, D.; Kolis, J. *Acta Crystallogr.* **2009**, *B65*, 445.
(8) Chen, C.; Bai, L.; Wang, Z.; Li, R. *J. Cryst. Growth* **2006**, *292*, 169.
(9) Chen, C.; Wu, Y.; Jiang, A.; Wu, B.; You, G.; Li, R.; Lin, S. *J. Opt. Soc. Am.* **1989**, *B6*, 616.
(10) Keszler, D. A. *Curr. Opin. Solid State Mater. Sci.* **1996**, *1*, 204.
(11) Giesber, H.; Ballato, J.; Chumanov, G.; Kolis, J.; Dejneka, M. *J. Appl. Phys.* **2003**, *93*, 8987.
(12) McMillen, C.; Kolis, J. *Inorg. Chem.* **2011**, *50*, 6809.
(13) McMillen, C.; Heyward, C.; Giesber, H.; Kolis, J. *J. Solid State Chem.* **2011**, *184*, 2966.
(14) Sheldrick, G. M. *SHELXTL Version 6.1, Program for Crystal Structure Refinement*; University of Gottingen: Gottingen, Germany, 2000.
(15) Spek, A. L. *PLATON, A Multipurpose Crystallographic Tool*; Utrecht University: Utrecht, The Netherlands, 2003.
(16) Grice, J. D.; Burns, P. C.; Hawthorne, F. C. *Can. Mineral.* **1999**, *37*, 731.
(17) Hawthorne, F. C.; Burns, P. C.; Grice, J. D. *Boron: Mineralogy, Petrology and Geochemistry*; Reviews in Mineralogy; Grew, E. S., Anovitz, L. M., Eds.; Mineralogical Society of America: Washington, DC, 2002; Vol. 33, pp 41−116.
(18) Filatov, S. K; Bubnova, R. S. *Glass Phys. Chem.* **2000**, *41*, 216.
(19) Ghose, S. *Am. Mineral.* **1982**, *67*, 1265.
(20) Smith, R.; Keszler, D. A. *J. Solid State Chem.* **1989**, *81*, 305.
(21) Shannon, R. D. *Acta Crystallogr.* **1976**, *A32*, 751.
(22) Burns, P. C.; Hawthorne, F. C. *Can. Mineral.* **1993**, *31*, 297.
(23) Burns, P. C.; Hawthorne, F. C. *Can. Mineral.* **1994**, *32*, 895.
(24) Yu, D.; Xue, D.; Ratajczak, H. *J. Mol. Struct.* **2006**, *783*, 210.
(25) Brese, N. E.; O'Keeffe, M. *Acta Crystallogr.* **1991**, *B47*, 192.
(26) Ross, S. D. In *The Infrared Spectra of Minerals*; Farmer, V. C., Ed.; Mineralogical Society Monograph 4; Mineralogical Society: London, 1974; pp 205−226.
(27) Weir, C. E. *J. Res. Natl. Bur. Stand.* **1966**, *70A*, 153.
(28) Jun, L.; Shuping, X.; Shiyang, G. *Spectrochim. Acta* **1995**, *A51*, 519.